DOI 10.2478/ama-2025-0039

NATURAL FREQUENCIES OF FUNCTIONALLY GRADED SANDWICH PLATES RESTING ON AN ELASTIC FOUNDATION USING CHEBYSHEV FINITE ELEMENT METHOD

Hoang Lan TON-THAT*

*Department of Civil Engineering, HCM city University of Architecture, 196 Pasteur, District 3, Ho Chi Minh, Vietnam

lan.tonthathoang@uah.edu.vn

received 21 January 2025, revised 16 April 2025, accepted 02 May 2025

Abstract: In this study, the article uses a finite element method based on Chebyshev polynomials to calculate the natural frequencies of functionally graded sandwich (FGS) plates with hard-core (HC) or soft-core (SC) resting on an elastic foundation. Chebyshev polynomials are a series of orthogonal polynomials defined recursively, and the value of them belongs to the range [-1, 1] as well as vanishes at Gauss points. More clearly, the novelty of this article is to use the high-order shape functions that satisfy the interpolation condition at the points based on Chebyshev polynomials to build the flat quadrilateral element for analysis of FGS plates. On the other hand, these plates are composed of two functionally graded skins and a hard or soft core. The elastic foundation with a two-parameter as a spring stiffness (α_1) and a shear layer stiffness (α_2) are used. Comparative examples are presented to validate the effectiveness of the current approach.

Key words: functionally graded sandwich plate, frequency, Chebyshev polynomial, finite element method, elastic foundation

1. INTRODUCTION

Nowadays, sandwich plates are common and important components of engineering structures consisting of two skins integrated with a core. These structures stand out for their outstanding bending stiffness, low mass density, efficient noise cancellation, and thermal insulation. They could be widely applied in many fields of engineering and defense technology. However, they also exhibit shortcomings, such as susceptibility to damage due to stress concentration or material discontinuities. Therefore, studying their mechanical behavior is necessary and has practical significance in engineering. Some typical deformation theories proposed and applied to analyze sandwich structures are the first-order shear deformation theory [1-3], the higher-order shear deformation theory [4-7], or the quasi-3D theory [8, 9], and many refined theories [10-17]. Furthermore, readers can find some results on sandwich structure analysis as well as composite structures in available documents [15-24]. For example, in the document [1], the authors presented analytical solutions for free vibration analysis of moderately thick rectangular plates, which were composed of functionally graded materials and supported by either Winkler or Pasternak elastic foundations. Based on the first-order shear deformation plate theory, the analysis procedure solved the exact equations of motion and captured the fundamental frequencies of the functionally graded rectangular plates resting on an elastic foundation. Theoretical formulation, Navier's solutions of rectangular plates, and finite element models based on the third-order shear deformation plate theory were presented in [2] for the analysis of through-thickness functionally graded plates. A refined trigonometric higher-order plate theory as in [3] was presented for bending analysis of simply supported functionally graded ceramic-metal sandwich plates. The effects of transverse shear strains as well as the transverse normal strain were taken into account. The number of unknown functions was only four, as opposed to six or more in the case of other shear and normal deformation theories. A general third-order plate theory that accounts for geometric nonlinearity and two constituent material variations through the plate thickness (i.e., functionally graded plates) was presented using the dynamic version of the principle of virtual displacements. The formulation was based on power-law variation of the material through the thickness and the von Kármán nonlinear strains. The governing equations of motion derived herein for a general third-order theory with geometric nonlinearity and material gradation through the thickness were specialized to the existing classical and shear deformation plate theories in the literature. Analysis of functionally graded material plates was studied using higher-order shear deformation theory with some special modifications in conjunction with finite element models [4-7]. Furthermore, the vibrational or thermomechanical bending behaviors of functionally graded sandwich plates were also presented in the documents [8-10]. Quasi-3D plate theories considering shear and normal deformations were incorporated to estimate the final results. In the papers [11, 12], the bending and the free flexural vibration behavior of sandwich functionally graded material plates were investigated based on higher-order structural theory. This theory accounted for the realistic variation of the displacements through the thickness. A multi-layered shell formulation was developed in the paper [13] based on a layerwise deformation theory within the framework of isogeometric analysis. The high-order smoothness of non-uniform rational B-splines offered the opportunity to capture the structural deformation efficiently in a rotation-free manner. The derivation also followed a layerwise theory, which assumed a separate displacement field expansion within each layer and considered the transverse displacement component as C0-continuous at layer interfaces, thus resulting in a layerwise

DOI 10.2478/ama-2025-0039

continuous transverse strain state. In the paper [14], the authors derived a higher-order shear deformation theory for modeling functionally graded plates accounting for extensibility in the thickness direction. The explicit governing equations and boundary conditions were obtained using the principle of virtual displacements under Carrera's Unified Formulation. The static and eigenproblems were solved by collocation with radial basis functions.

In recent years, the study of structures embedded in foundations has drawn a lot of attention amongst researchers. To express the interaction between foundation and plate, various hypotheses of foundation models have been introduced [15]. The oldest and simplest hypothesis of elastic medium models, which has only one coefficient substrate reaction, is known as Winkler elastic foundation [16]. Despite its ease of implementation, the Winkler model is defective in providing continuity in the foundation due to separate springs [17]. This hypothesis was improved by the Pasternak model [18] via adding a shear layer over springs. The Pasternak model, including two-parameter substrate (spring and shear layer), is widely used to explain the mechanical interactions of soft plates with different distributions of material properties. In the Kerr foundation [19], nonconcentrated reactions do not occur due to an upper spring layer. It means that, in the Kerr model, a shear layer is surrounded by upper and lower spring layers. From there one can see more related documents. The thermodynamic behavior of functionally graded sandwich plates resting on Winkler/Pasternak/Kerr foundations with various boundary conditions was studied in [20] by using a refined 2D plate theory. The displacement field contained undetermined integral forms and involved only four unknowns to derive. The plate was considered to be subject to a time-harmonic sinusoidal temperature field across its thickness. Three types of foundations were studied. Each was described by a mathematical model. Different boundary conditions were used to study the thermodynamic behavior of sandwich plates on elastic foundations. These models gave an incredible concurrence with the accessible literature. The research [21] investigated the free vibration analysis of advanced composite plates, such as functionally graded plates resting on two-parameter elastic foundations, using a hybrid quasi-3D (trigonometric as well as polynomial) higher-order shear deformation theory. The theory, which did not require a shear correction factor, accounted for shear deformation and thickness stretching effects by a sinusoidal and parabolic variation of all displacements across the thickness. The governing equations of motion for the plates were derived from Hamilton's principle. The closed-form solutions were obtained by using the Navier technique, and natural frequencies were found for simply supported plates by solving the results of eigenvalue problems. The research [22] analyzed the natural frequencies of the imperfect functionally graded sandwich plate comprised of porous face sheets made of functionally graded materials and an isotropic homogeneous core resting on the elastic foundation. To accomplish this, the material characteristics were taken to be changed incessantly along the thickness direction based on the volume fraction of constituents expressed by the modified rule of the mixture, which included porosity volume fraction with three diverse kinds of porosity distribution models. Furthermore, to describe the two-parameter elastic foundation's response on the imperfect plates, the medium was supposed to be linear, homogenous, and isotropic, and it had been modeled using the Winkler-Pasternak model. Moreover, in the kinematic relationship of the imperfect plate resting on the Winkler-Pasternak foundation, third-order shear deformation theory was used, and the motion equations were set up employing Hamilton's principle. A buckling analysis of functionally graded plates of a complex form resting on an elastic foundation and subjected to an in-plane nonuniform loading was performed by the R-functions method as in [23]. The mathematical formulation of the problem was presented within the framework of the classical laminate plate theory. The approach proposed and the software developed consider the heterogeneous subcritical state of the plates. To solve the problems, the Ritz method combined with the R-functions theory was used, etc.

Another aspect: the finite element method was first introduced in 1960 with the basic idea of dividing the entire problem domain into discrete components with simple geometry. Within each element, the representation of dependent variables is accomplished through shape functions. Structural analysis using the finite element method will be more accurate with higher-order shape functions. Nowadays, applying the finite element method to structural analysis has become popular and shows outstanding benefits compared to analytical methods, especially for structures with complex shapes and arbitrary boundary conditions. The study [24] focused on establishing the finite element model based on a new hyperbolic shear deformation theory to investigate the static bending, free vibration, and buckling of the functionally graded sandwich plates with porosity. The novel sandwich plate consisted of one homogenous ceramic core and two different functionally graded face sheets, which could be widely applied in many fields of engineering and defense technology. The discrete governing equations of motion were carried out via Hamilton's principle and the finite element method. Besides, Chebyshev polynomials play a significant role in approximation theory. They constitute a sequence of orthogonal polynomials defined recursively. Their absolute value in the interval [-1, 1] is bounded by 1. Based on this ideal, the authors [25, 26] proposed a finite element method associated with Chebyshev polynomials of the first kind for the analysis of plate/shell structures. In this approach, Gauss points were employed to formulate the shape functions grounded in Chebyshev polynomials. Consequently, the code was introduced to overcome shear locking and eliminate spurious zero energy modes.

There are different approaches to analyzing this type of structure, and in this article, the finite element method based on Chebyshev polynomials is first used to study the free vibration of FGS plates with HC or SC resting on an elastic foundation. The reliability of this method is verified through numerical examples related to the effects of geometrical parameters, materials, and foundation. Furthermore, increasing the degree of the Chebyshev polynomial will increase the total number of degrees of freedom of the structure, leading to increased computational costs. However, the survey in this paper shows that it is possible to control the degree of the polynomial sufficiently to obtain the required approximate results. Some other advantages of the proposed method, although not explicitly verified in this article, are that the obtained results are not affected by mesh distortion or, although the Chebyshev interpolation polynomial is established in the form of the Lagrange interpolation, Runge's phenomenon [27] does not occur; therefore, it can be used as an original finite element method for solving PDEs with high accuracy.

This article is organized as follows. The formulation is presented in Sect. 2. To highlight the reliability of the element, some numerical examples are thoroughly studied in Sect. 3. Finally, conclusions are drawn in Sect. 4.

2. FORMULATION

Considering rectangular FGS plates with HC or SC resting on an elastic foundation as shown in Fig. 1. A group of $h_1 - h_2 - h_3$

DOI 10.2478/ama-2025-0039

represents the ratio of thicknesses.

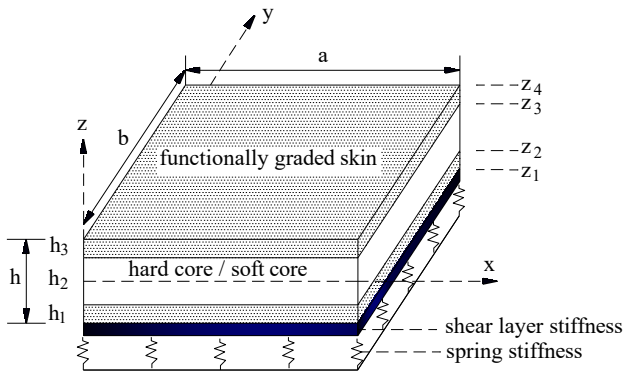

Fig. 1. The model of an FGS plate resting on an elastic foundation

The volume fraction $V_c^{(i)}$ of the ceramic phase of each layer is formulated by [3]

+ For FGS plate with HC (FGS-HC):

$$\begin{cases} V_c^{(1)} = \left(\frac{z-z_1}{z_2-z_1}\right)^n & z \in [z_1, z_2] \\ V_c^{(2)} = 1 & z \in [z_2, z_3] \\ V_c^{(3)} = \left(\frac{z-z_4}{z_3-z_4}\right)^n & z \in [z_3, z_4] \end{cases} \quad (1)$$

+ For FGS plate with SC (FGS-SC):

$$\begin{cases} V_c^{(1)} = 1 - \left(\frac{z-z_1}{z_2-z_1}\right)^n & z \in [z_1, z_2] \\ V_c^{(2)} = 0 & z \in [z_2, z_3] \\ V_c^{(3)} = 1 - \left(\frac{z-z_4}{z_3-z_4}\right)^n & z \in [z_3, z_4] \end{cases} \quad (2)$$

The effective material properties of FGS plates are determined by

$$M^{(i)}(z) = M_c V_c^{(i)} + M_m(1 - V_c^{(i)}), \quad i = 1,2,3 \quad (3)$$

Here $M^{(i)}(z)$ stands for the material characteristics of each layer.

a) FGS-HC

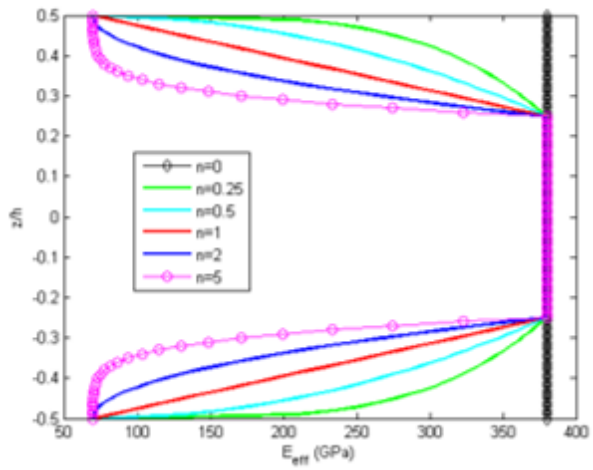

b) FGS-SC

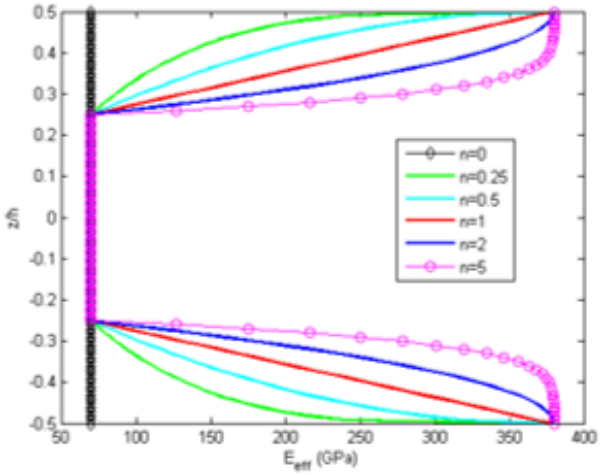

Fig. 2. The effective elastic modulus against the thickness of (Al/Al_2O_3)_FGS_(1-2-1) plates

The mechanical characteristics of the ceramic and metal are used in this article as Al_2O_3 (E = 380 GPa, ρ = 3800 kg/m^3, ν = 0.3); Al (E = 70 GPa, ρ = 2707 kg/m^3, ν = 0.3); and ZrO_2 (E = 151 GPa, ρ = 3000 kg/m^3, ν = 0.3). In addition, Fig. 2 plots the effective elastic modulus versus the thickness of (Al/Al_2O_3)_FGS_(1-2-1).

The elastic foundation is modeled with two parameters (α_1, α_2). The foundation reaction is given as a function of the deflection and its Laplacian. The reaction-deflection relation of this foundation is defined by

$$\Re = \alpha_1 w - \alpha_2 \left(\frac{\partial^2 w}{\partial x^2} + \frac{\partial^2 w}{\partial y^2}\right) \quad (4)$$

The Chebyshev polynomials as in [25, 26] is given

$$C_p(x) = C_p(\cos\varphi) = \cos p\varphi, \quad x = \cos\varphi \in [-1,1] \quad (5)$$

$$\cos(p+1)\varphi = 2\cos\varphi \cos p\varphi - \cos(p-1)\varphi \quad (6)$$

or

$$C_{p+1}(x) = 2xC_p(x) - C_{p-1}(x), \quad p = 0,1,2\ldots \quad (7)$$

The Chebyshev polynomial $C_p(x)$with $p \geq 2$will equals 0 at the Gauss points x_i

$$x_i = -\cos[(2i-1)\pi/2p], \quad i = 1,2,3,\ldots \quad (8)$$

The most important of ideas involves the approximation process of an unknown function $f(x)$ by Lagrangian interpolation polynomial $\aleph(x)$ through these known points $(x_k, f(x_k))$ based on Chebyshev polynomials as described

$$f(x) \approx \aleph(x) = \sum_{i=0}^{p-1} a_i C_i(x) \quad and \quad f(x_k) = \aleph(x_k) \quad (9)$$

On the interval [-1, 1], Chebyshev polynomials have the orthogonal property so the unknown coefficient $a_i$may be calculated by

$$a_i = \sum_{k=1}^{p} f(x_k) C_i(x_k) / \sum_{k=1}^{p} C_i^{\,2}(x_k) \quad (10)$$

Hence

$$\aleph(x) = \sum_{k=1}^{p} \sum_{i=0}^{p-1} \left[\left(C_i(x_k) C_i(x)\right) / \sum_{j=1}^{p} C_i^2(x_j)\right] f(x_k) \quad (11)$$

with $x = \cos(\pi/2p)\,\xi$

$$\aleph(\xi) = \sum_{k=1}^{p} N_k(\xi)\, f(\xi_k) \quad (12)$$

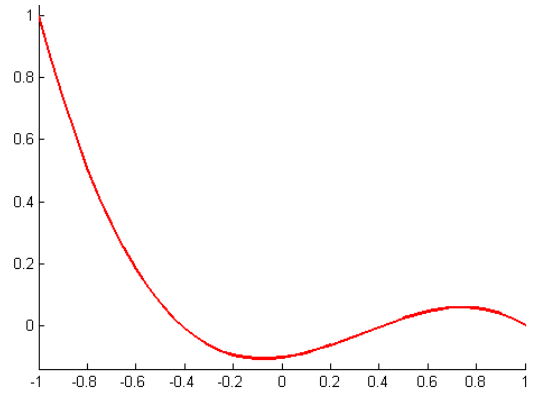

$N_1(\xi)$

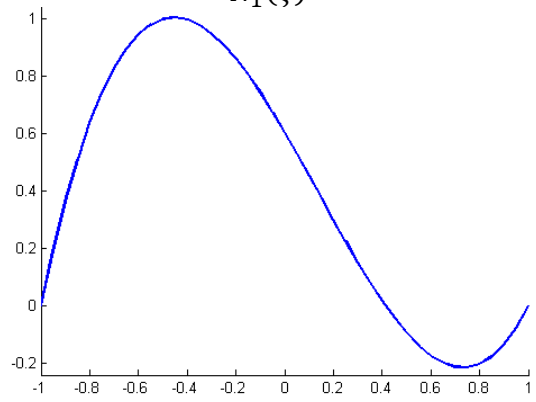

$N_2(\xi)$

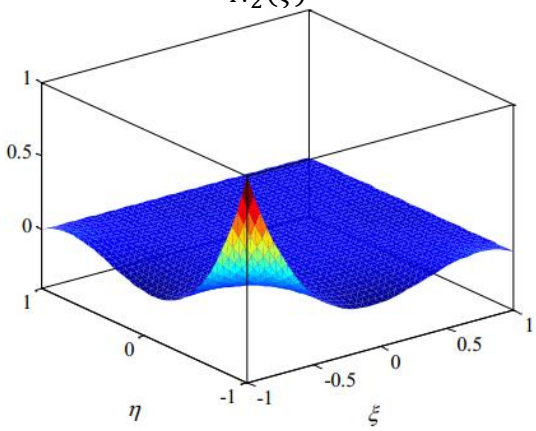

$\widetilde{N}_1(\xi,\eta)$

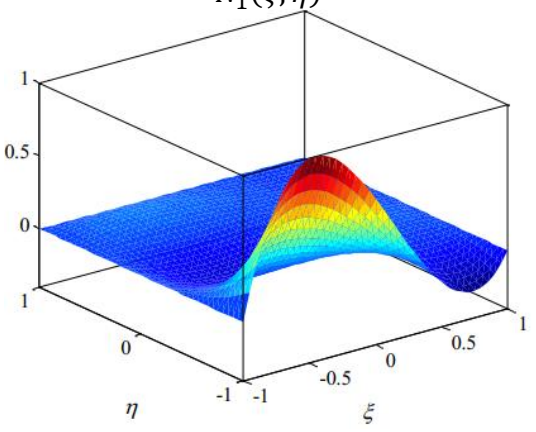

$\widetilde{N}_2(\xi,\eta)$

Fig. 3. The third-order shape functions in 1D & 2D

where $N_k(\xi)$ are called the 1D shape functions defined as

$$N_k(\xi) = \sum_{i=0}^{p-1} \left[\left(C_i(cos(\pi/2p)\,\xi_k) C_i(cos(\pi/2p)\,\xi) \right) / \sum_{j=1}^{p} C_i^2(cos(\pi/2p)\,\xi_j) \right] \quad (13)$$

$$\xi_i = -cos[(2i-1)\pi/2p] \,/\, cos(\pi/2p) \qquad i = 1,2,\ldots,p \quad (14)$$

In 2D problems, $(\xi,\eta) \in [-1,1] \times [-1,1]$, the shape functions associated with node $K(\xi_i,\eta_j)$

$$\widetilde{N}_K(\xi,\eta) = N_i(\xi) N_j(\eta) \quad (15)$$

with $N_i(\xi)$ or $N_j(\eta)$ is 1D *p*-order shape functions related to the set $\xi \in [-1,1]$ or the set $\eta \in [-1,1]$ respectively. Fig. 3 gives some third-order shapes functions related to the Chebyshev polynomials in 1D space and 2D space.

The finite element formulation related to Chebyshev polynomials is established as in [25, 26]. The plate is divided by the quadrilateral elements with five degrees of freedom in each node of an element. These components can be approximated through the displacement components at node *K*

$$u = \underset{(p+1)(q+1)}{\{u_o \quad v_o \quad w_o \quad \beta_x \quad \beta_y\}^T} = \sum_{K=1} \widetilde{N}_K(\xi,\eta) \{u_{oK} \quad v_{oK} \quad w_{oK} \quad \beta_{xK} \quad \beta_{yK}\}^T = N_K d_K \quad (16)$$

with

$$N_K = \widetilde{N}_K diag(1,1,1,1,1),$$

$$d_K = \{u_{oK} \quad v_{oK} \quad w_{oK} \quad \beta_{xK} \quad \beta_{yK}\}^T$$

are nodal displacement vector associated node *K*. Based on the first-order shear deformation theory, the kinematics of the plate is calculated through five displacement components u_o, v_o, w_o, β_x and β_y in the mid-surface

$$u(x,y,z) = u_0(x,y) + z\beta_x$$
$$v(x,y,z) = v_0(x,y) + z\beta_y \quad (17)$$
$$w(x,y,z) = w_0(x,y)$$

with u_o, v_o, w_o are three displacement components, and β_x β_y are the rotations related to the *x*- and *y*- axes. The in-plane strain vector and the transverse shear strain vector are shown

$$\varepsilon = \begin{bmatrix} \varepsilon_{xx} \\ \varepsilon_{yy} \\ \gamma_{xy} \end{bmatrix} = \underbrace{\begin{bmatrix} u_{0,x} \\ v_{0,y} \\ u_{0,y} + v_{0,x} \end{bmatrix}}_{\varepsilon^m} + z \underbrace{\begin{bmatrix} \beta_{x,x} \\ \beta_{y,y} \\ \beta_{x,y} + \beta_{y,x} \end{bmatrix}}_{\varepsilon^b} \quad (18)$$

$$= \varepsilon^m + z\varepsilon^b$$

$$\varepsilon^s = \begin{bmatrix} \gamma_{xz} \\ \gamma_{yz} \end{bmatrix} = \begin{bmatrix} \beta_x + w_{0,x} \\ \beta_y + w_{0,y} \end{bmatrix} \quad (19)$$

The constitutive relation for functionally graded plate can be defined as below

$$\begin{Bmatrix} \sigma_{xx} \\ \sigma_{yy} \\ \tau_{xy} \\ \tau_{xz} \\ \tau_{yz} \end{Bmatrix} = \begin{bmatrix} Q_{11} & Q_{12} & 0 & 0 & 0 \\ Q_{21} & Q_{22} & 0 & 0 & 0 \\ 0 & 0 & Q_{66} & 0 & 0 \\ 0 & 0 & 0 & Q_{55} & 0 \\ 0 & 0 & 0 & 0 & Q_{44} \end{bmatrix} \begin{Bmatrix} \varepsilon_{xx} \\ \varepsilon_{yy} \\ \gamma_{xy} \\ \gamma_{xz} \\ \gamma_{yz} \end{Bmatrix} \quad (20)$$

with the material constants are given by

DOI 10.2478/ama-2025-0039

$$Q_{11} = Q_{22} = E(z)/[1-\nu^2(z)],$$
$$Q_{12} = Q_{21} = \nu(z)E(z)/[1-\nu^2(z)], \quad (21)$$
$$Q_{44} = Q_{55} = Q_{66} = E(z)/2[1+\nu(z)]$$

By applying the Hamilton's principle, the weak-form for free vibration analysis can be presented by

$$\int_\Omega \delta\bar{\varepsilon}^T D_b^* \bar{\varepsilon} d\Omega + \int_\Omega \delta\bar{\gamma}^T D_s^* \bar{\gamma} d\Omega + \int_\Omega \Re w \, d\Omega = \int_\Omega \delta u^T m\ddot{u} \, d\Omega \quad (22)$$

where

$$\bar{\varepsilon} = \{\varepsilon^m, \varepsilon^b\}^T, \qquad \bar{\gamma} = \{\varepsilon^s\}^T \quad (23)$$

and $m = \begin{bmatrix} I_1 & I_2 \\ I_2 & I_3 \end{bmatrix}$ with the mass inertia terms $I_i (i = 1,2,3)$ are given by

$$(I_1, I_2, I_3) = \int_{-h/2}^{h/2} \rho(z)\,(1, z, z^2) \begin{bmatrix} 1 & 0 & 0 \\ 0 & 1 & 0 \\ 0 & 0 & 1 \end{bmatrix} dz \quad (24)$$

Besides, D_b^* and D_s^*, the material matrices, are written by

$$D_b^* = \begin{bmatrix} A & B \\ B & D \end{bmatrix}, \quad D_s^* = A^s \quad (25)$$

with

$$(A, B, D) = \int_{-h/2}^{h/2} (1, z, z^2) \begin{bmatrix} Q_{11} & Q_{12} & 0 \\ Q_{21} & Q_{22} & 0 \\ 0 & 0 & Q_{66} \end{bmatrix} dz,$$
$$A^s = \frac{5}{6} \int_{-h/2}^{h/2} \begin{bmatrix} Q_{55} & 0 \\ 0 & Q_{44} \end{bmatrix} dz \quad (26)$$

The discretized systems for free vibration analysis may be given as

$$(K - \omega^2 M)d = 0 \quad (27)$$

where $K$is the global stiffness matrix including the plate and elastic foundation, M is the global mass matrix, respectively. Furthermore, the Gauss quadrature rule is taken on the integration through a set of (p+1)(q+1) Gauss points, in which p and q are the orders of $N_i(\xi)$and $N_j(\eta)$. The total numbers of Gauss points and degrees of freedom per each element are (p+1)(q+1) and 5(p+1)(q+1). The values of p and q are set to 3 for all numerical examples by following [16]. The BCs are given by

Clamped (C): $u_0 = v_0 = w_0 = \beta_x = \beta_y = 0$ at all edges.

Simply supported (S): $u_0 = w_0 = \beta_x = 0$ at $y = 0$ & y = b and $v_0 = w_0 = \beta_y = 0$ at $x = 0$ & x = a.

In order to clarify how the proposed technique is incorporated into a finite element code, a numerical implementation is briefly presented as follows.

- Discretize the domain into quadrilateral elements and form the matrices of node coordinates (*coord*) and element connections (*nodes*).
- Declare the order p, q of the Chebyshev polynomials. The Gauss quadrature rule is taken on the integration through a set of (p+1)(q+1) Gauss points.
- Calculate and assemble element matrices to build the system matrices.
- Assign boundary conditions.
- Solve the system of equations to obtain results.

3. NUMERICAL RESULTS AND DISCUSSIONS

The normalized parameters in this study are expressed by

$$k_1 = \alpha_1 a^4/D_m, \quad k_2 = \alpha_2 a^2/D_m,$$
$$D_m = E_m h^3/12/(1-\nu_m^2),$$
$$\bar{\omega} = \left(\frac{\omega a^2}{h}\right)\sqrt{\frac{\rho_o}{E_o}}, \quad (28)$$
$$\rho_o = 1kg/m^3, \quad E_o = 1GPa$$

Firstly, the free vibration analysis of thin (h = a/200) and thick (h = a/10) square plates with two boundary conditions, SSSS and CCCC, is considered. The Young's modulus E = 200 GPa, Poisson ratio ν = 0.3, and mass density ρ = 8000 kg/m^3 are the material properties. The first four normalized frequencies of these structures $\omega^* = [12\omega\rho a^4(1-\nu^2)/(Eh^2)]^{1/4}$are presented in Table 1 and Fig. 4. These results are also compared with other results of MITC4 element [28] and exact solutions [29].

Tab. 1. The first four normalized frequencies of square plate (h = a/10, a/200)

Mode	a/h = 10, (SSSS)		
	[28]	Article	[29]
1	4.403	4.366	4.37
2	6.940	6.744	6.74
3	6.940	6.744	6.74
4	8.608	8.354	8.35
Mode	**a/h = 10, (CCCC)**		
	[28]	**Article**	**[29]**
1	5.808	5.703	5.71
2	8.226	7.876	7.88
3	8.226	7.876	7.88
4	9.731	9.325	9.33
Mode	**a/h = 200, (SSSS)**		
	[28]	**Article**	**[29]**
1	4.481	4.443	4.443
2	7.252	7.025	7.025
3	7.252	7.025	7.025
4	9.200	8.885	8.886
Mode	**a/h = 200, (CCCC)**		
	[28]	**Article**	**[29]**
1	6.124	5.998	5.999
2	9.060	8.567	8.568
3	9.060	8.567	8.568
4	11.019	10.403	10.407

Tab. 2. The first frequency of FGM plates resting on the elastic foundation with n = 1 and h = a/20

(k_1, k_2)	Method	p=q	Meshing		
			4 x 4	6 x 6	8 x 8
(100,100)	Article	1	0.0662	0.0510	0.0474
		2	0.0398	0.0397	0.0396
		3	0.0396	0.0396	0.0396
		4	0.0396	0.0396	0.0396
	[30]		0.0388		
	[31]		0.0386		

Tab. 3. The dimensionless frequencies of the FGS-HC plate resting on the elastic foundation.

a/h	*n*	(k_1, k_2)	(2-1-2)		(1-1-1)		(2-2-1)	
			Article	[32]	Article	[32]	Article	[32]
10	0	(0,0)	1.29918	1.29692	1.29918	1.29692	1.29918	1.29692
		(10,10)	1.61828	1.61603	1.61828	1.61603	1.61828	1.61603
		(100,100)	3.32217	3.31161	3.32217	3.31161	3.32217	3.31161
	10	(0,0)	0.93921	0.93742	0.95419	0.95372	0.98414	0.98239
		(10,10)	1.37299	1.37067	1.38093	1.37733	1.40154	1.39522
		(100,100)	3.30716	3.29462	3.30545	3.2805	3.30531	3.28023
100	0	(0,0)	1.34067	1.34038	1.34067	1.34038	1.34067	1.34038
		(10,10)	1.65962	1.65899	1.65962	1.65899	1.65962	1.65899
		(100,100)	3.36947	3.36942	3.36947	3.36942	3.36947	3.36942
	10	(0,0)	0.96026	0.96023	0.97591	0.97582	1.00790	1.00620
		(10,10)	1.39691	1.39670	1.40294	1.40285	1.42311	1.42192
		(100,100)	3.34844	3.34801	3.33422	3.33315	3.33346	3.33266

a) Thin plate

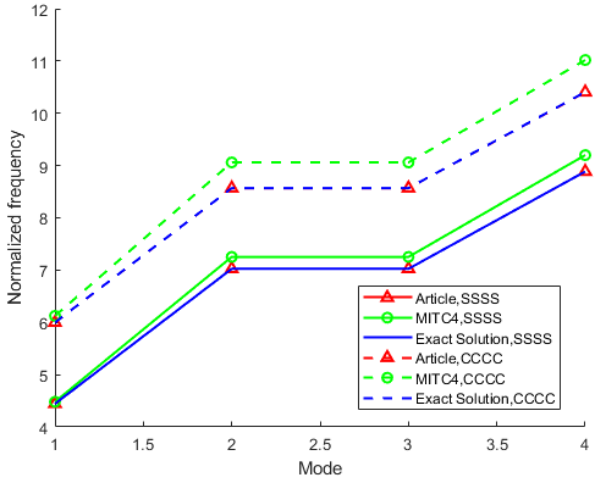

b) Think plate

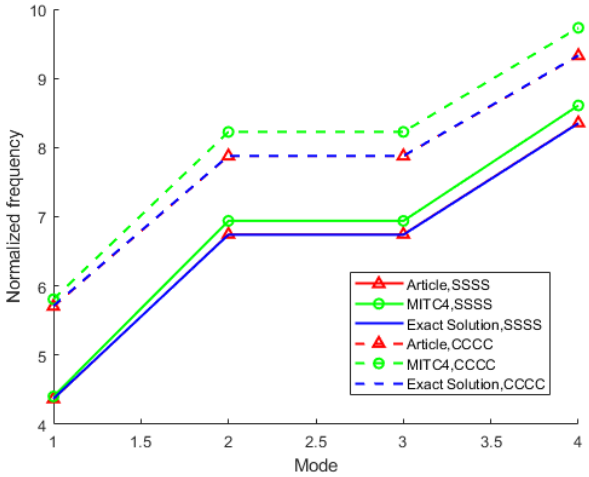

Fig. 4. The comparison of the first four normalized frequencies of square plate

Secondly, consider the SSSS square (*Al/Al*$_2$*O*$_3$) FGM plate resting on an elastic foundation. The dimensionless frequency is normalized by

$$\omega^{**} = (\omega h)\sqrt{\rho_b / E_b}.$$

Observing that the obtained results converge at a mesh size of 4 × 4 with the order of shape functions $p = q = 3$ and are in good agreement with those of solutions using quasi-3D theory [30] and third-order shear deformation theory [31], as given in Table 2. An error of about 2% compared to the results from quasi-3D theory is acceptable when using only coarse meshes.

Next, the SSSS square (*Al/ZrO*$_2$) FGS-HC plate is considered. The first normalized frequencies $\bar{\omega}$ are provided in Table 3. It can be observed that the obtained results are completely consistent with the results of [32], employing a closed-form solution based on the hyperbolic shear deformation theory. Moreover, it is clear from the table that the natural frequencies are increasing with the existence of the elastic foundation. Clearly, the natural frequencies are increasing with the increasing values of two parameters: spring stiffness and shear layer stiffness. Table 3 also shows that, as the volume ratio of ceramic in the sandwich plate increases, the natural frequencies of the plate increase.

Continuously, the dimensionless frequencies of the square (Al/ZrO2) FGS plates with different values of the power-law index, ratio of thicknesses, and BCs are listed in Table 4 and Table 5. From these tables, it can be seen that when the power-law index n increases, the frequencies of the FGS-HC plates decrease while the frequencies of the FGS-SC increase. The reason is that as n increases, the volume fraction of ceramic decreases for the FGS-HC plate, leading to a decrease in the FGS-HC plate stiffness; so the frequency of the FGS plate decreases. The frequency of FGS-HC plates with n = 0 is highest, because when n = 0, FGS-HC plates become homogeneous ceramic plates. On the other hand, when n increases, the frequencies of the FGS-SC plates increase, because when n increases, the volume fraction of the ceramic components increases, and the FGS plate stiffness increases. Besides, when n = 0, the FGS-SC plates become homogeneous metal plates, so the frequency of FGS plates is the smallest. In addition, the thicker ceramic core results in a stiffer FGS-HC plate, causing the frequency of the FGS plate to increase. This is in contrast to the FGS-SC plate, when the thicker metal core leads to a softer FGS-SC plate, so the frequency of the FGS plates reduces.

Tab. 4. The dimensionless frequencies of square FGS plates with $a/h = 15$, $k_1 = 10$, $k_2 = 10$

BCs	Plate	*n*	Ratio of thicknesses			
			(1-0-1)	(1-1-1)	(1-2-2)	(1-6-1)
SSSS	FGS-HC	0	1.9543	1.9543	1.9543	1.9543
		0.5	1.5924	1.6596	1.6907	1.8175
		1	1.4114	1.5053	1.5556	1.7477
		2	1.2580	1.3579	1.4278	1.6794
		5	1.1721	1.2350	1.3213	1.6209
		10	1.1662	1.1949	1.2819	1.6067
	FGS-SC	0	1.1769	1.1769	1.1769	1.1769
		0.5	1.7605	1.6906	1.6537	1.4641
		1	1.8992	1.8417	1.7978	1.5740
		2	1.9714	1.9446	1.8989	1.6657
		5	1.9852	2.0037	1.9611	1.7343
		10	1.9733	2.0155	1.9776	1.7504
SSCC	FGS-HC	0	2.5957	2.5957	2.5957	2.5957
		0.5	2.0944	2.1903	2.2334	2.4092
		1	1.8388	1.9751	2.0455	2.3131
		2	1.6161	1.7658	1.8655	2.2194
		5	1.4846	1.5889	1.7125	2.1385
		10	1.4699	1.5283	1.6548	2.1181
	FGS-SC	0	1.4774	1.4774	1.4774	1.4774
		0.5	2.3060	2.2035	2.1516	1.8838
		1	2.5018	2.4142	2.3537	2.0374
		2	2.6067	2.5587	2.4952	2.1638
		5	2.6317	2.6435	2.5834	2.2584
		10	2.6188	2.6624	2.6087	2.2805
SCSC	FGS-HC	0	2.7507	2.7507	2.7507	2.7507
		0.5	2.2165	2.3197	2.3655	2.5530
		1	1.9420	2.0896	2.1641	2.4509
		2	1.7015	1.8651	1.9717	2.3510
		5	1.5573	1.6737	1.8071	2.2649
		10	1.5398	1.6082	1.7447	2.2430
	FGS-SC	0	1.5457	1.5457	1.5457	1.5457
		0.5	2.4340	2.3225	2.2671	1.9804
		1	2.6444	2.5476	2.4825	2.1437
		2	2.7581	2.7025	2.6345	2.2782
		5	2.7871	2.7944	2.7302	2.3788
		10	2.7747	2.8154	2.7575	2.4024
CCCC	FGS-HC	0	3.3663	3.3663	3.3663	3.3663
		0.5	2.7033	2.8327	2.8898	3.1229
		1	2.3590	2.5461	2.6399	2.9967
		2	2.0540	2.2641	2.3985	2.8727
		5	1.8669	2.0222	2.1906	2.7658
		10	1.8407	1.9381	2.1113	2.7389
	FGS-SC	0	1.8436	1.8436	1.8436	1.8436
		0.5	2.9587	2.8163	2.7473	2.3877
		1	3.2223	3.0967	3.0158	2.5904
		2	3.3669	3.2904	3.2055	2.7581
		5	3.4070	3.4069	3.3268	2.8827
		10	3.3937	3.4346	3.3620	2.9119

Tab. 5. The first four frequencies of square FGS plates (1-4-1) with $a/h = 45$, $k_1 = 50$, $k_2 = 15$

BCs	Plate	*n*	Normalized frequencies			
			$\bar{\omega}_1$	$\bar{\omega}_2$	$\bar{\omega}_3$	$\bar{\omega}_4$
SSSS	FGS-HC	0	2.0351	4.8527	4.8527	7.6586
		0.5	1.8611	4.3877	4.3877	6.9055
		1	1.7707	4.1436	4.1436	6.5090
		2	1.6811	3.8982	3.8982	6.1097
		5	1.5964	3.6633	3.6633	5.7257
		10	1.5643	3.5740	3.5740	5.5797
	FGS-SC	0	1.3185	2.7594	2.7594	4.1886
		0.5	1.6503	3.7252	3.7252	5.7897
		1	1.7741	4.0725	4.0725	6.3581
		2	1.8764	4.3540	4.3540	6.8179
		5	1.9566	4.5755	4.5755	7.1788
		10	1.9831	4.6487	4.6487	7.2979
SSCC	FGS-HC	0	2.7052	5.9047	5.9266	8.9704
		0.5	2.4566	5.3292	5.3484	8.0838
		1	2.3269	5.0266	5.0448	7.6161
		2	2.1970	4.7216	4.7382	7.1440
		5	2.0732	4.4288	4.4437	6.6894
		10	2.0261	4.3177	4.3323	6.5166
	FGS-SC	0	1.6225	3.2659	3.2746	4.8327
		0.5	2.1214	4.4804	4.4956	6.7338
		1	2.3039	4.9129	4.9301	7.4055
		2	2.4527	5.2635	5.2827	7.9484
		5	2.5692	5.5387	5.5590	8.3744
		10	2.6083	5.6297	5.6504	8.5155
SCSC	FGS-HC	0	2.8756	5.3557	6.7353	9.1380
		0.5	2.6076	4.8374	6.0736	8.2344
		1	2.4671	4.5654	5.7249	7.7575
		2	2.3264	4.2913	5.3733	7.2769
		5	2.1921	4.0284	5.0346	6.8132
		10	2.1416	3.9287	4.9057	6.6368
	FGS-SC	0	1.6935	2.9985	3.6657	4.9129
		0.5	2.2376	4.0841	5.0755	6.8517
		1	2.4353	4.4723	5.5750	7.5362
		2	2.5967	4.7870	5.9794	8.0896
		5	2.7231	5.0344	6.2970	8.5240
		10	2.7652	5.1161	6.4020	8.6677
CCCC	FGS-HC	0	3.5315	7.1179	7.1179	10.4331
		0.5	3.1928	6.4172	6.4172	9.3997
		1	3.0152	6.0476	6.0476	8.8533
		2	2.8367	5.6747	5.6747	8.3016
		5	2.6652	5.3157	5.3157	7.7691
		10	2.6004	5.1788	5.1788	7.5661
	FGS-SC	0	2.0033	3.8544	3.8544	5.5549
		0.5	2.7066	5.3520	5.3520	7.7846
		1	2.9595	5.8820	5.8820	8.5694
		2	3.1644	6.3109	6.3109	9.2038
		5	3.3258	6.6474	6.6474	9.7021
		10	3.3789	6.7588	6.7588	9.8669

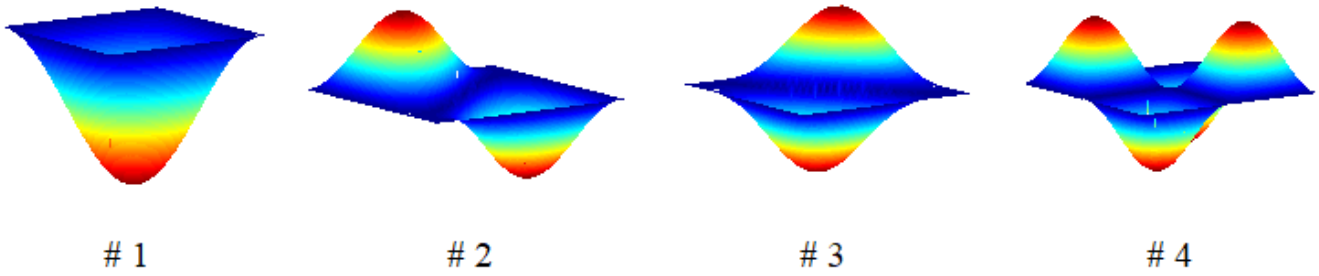

Fig. 5. The first four mode shapes of (SSSS) FGS-HC plate with $a/b = 1$, $a/h = 20$, $k_1 = 10$, $k_2 = 5$, $n = 1$, ratio of thicknesses (1-1-1)

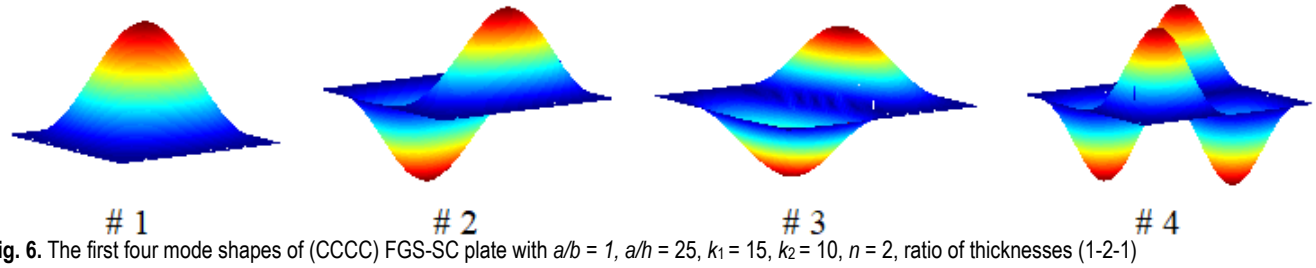

Fig. 6. The first four mode shapes of (CCCC) FGS-SC plate with $a/b = 1$, $a/h = 25$, $k_1 = 15$, $k_2 = 10$, $n = 2$, ratio of thicknesses (1-2-1)

Figs. 5 and 6 present the first four modeshapes of FGS plates. Observing that the 2nd and 3rd eigenmodes are the same as each other, owing to the FGS plates under the same "S" or "C" boundary conditions at the edges.

4. CONCLUSIONS

The article aims to conduct the frequency analysis of FGS plates resting on an elastic foundation by using a finite element method based on Chebyshev polynomials. The idea of this element is to use the high-order shape functions that satisfy the interpolation condition at the points based on Chebyshev polynomials as well as to use the full Gauss quadrature rule for the establishment of the stiffness matrix and mass matrix. Numerical examples and comments are made to illustrate in detail the influence of geometric parameters and material properties on the free vibrations of the FGS plates. According to the numerical outcomes, some important observations are summarized as follows: i. The effectiveness of using the finite element method based on Chebyshev polynomials in the analysis of free vibrations of FGS plates on the elastic foundation. ii. Elastic foundation increases the frequency of FGS plates, as expected. More specifically, the natural frequencies are increasing with the existence of an elastic foundation. The natural frequencies are increasing with the increasing values of two parameters: spring stiffness and shear layer stiffness. iii. While increasing the value of the power-law index leads to the decreasing value of the natural frequency for hardcore sandwich plates, the natural frequency increases with increasing value of the power-law index for softcore sandwich plates. In conclusion, it is evident that the elastic foundation has a significant effect on the mechanical behavior of sandwich plates.

The obtained results can be useful for extended calculation, design, and fabrication of FGS plates working under various conditions. In the near future, the proposed method will continue to demonstrate the stability of the results when meshing distortion. In addition, although the Chebyshev interpolation polynomial is established in the form of Lagrange interpolation, the Runge phenomenon does not occur, so it can be used as an original finite element method to solve PDEs with high accuracy. Besides, the task of nonlinear analysis of plate/shell structures will be developed. Last but not least, the computational cost for complex structures will also be considered to help readers have a specific view of the advantages and disadvantages of this proposed method.

REFERENCES

1. Hosseini HS, Taher HRD, Akhavan H, Omidi M. Free vibration of functionally graded rectangular plates using first-order shear deformation plate theory. Appl. Math. Model. 2010;34(5):1276-91. Available from: https://doi.org/10.1016/j.apm.2009.08.008
2. Reddy JN. Analysis of functionally graded plates. Int. J. Numer. Methods Eng. 2000;47:663-84.
3. Zenkour AM. Bending analysis of functionally graded sandwich plates using a simple four unknown shear and normal deformations theory. J. Sandw. Struct. Mater. 2013;15:629-56. Available from: https://doi.org/10.1177/1099636213498886
4. Reddy JN. A general nonlinear third-order theory of functionally graded plates. Int. J. Aerosp. Lightweight Struct. 2011;1:1-21. Available from: https://doi.org/10.3850/S201042861100002X
5. Talha M, Singh BN. Static response and free vibration analysis of FGM plates using higher order shear deformation theory. Appl. Math. Model. 2010;34:3991-4011.
Available from: https://doi.org/10.1016/j.apm.2010.03.034
6. Zenkour AM. Generalized shear deformation theory for bending analysis of functionally graded materials. Appl. Math. Model. 2006;30(1):67-84.
Available from: https://doi.org/10.1016/j.apm.2005.03.009
7. Yaghoobi H, Fereidoon A. Mechanical and thermal buckling analysis of functionally graded plates resting on elastic foundations: An assessment of a simple refined nth-order shear deformation theory. Compos. B: Eng. 2014;62:54-64. Available from: https://doi.org/10.1016/j.compositesb.2014.02.014
8. Sobhy M, Al-Mukahal FH. Magnetic control of vibrational behavior of smart FG sandwich plates with honeycomb core via a quasi 3D plate theory. Adv. Eng. Mater. 2023;25(13):2300096. Available from: https://doi.org/10.1002/adem.202300096
9. Zarga D, Tounsi A, Bousahla AA, Bourada F, Mahmoud SR. Thermomechanical bending study for functionally graded sandwich plates using a simple quasi-3D shear deformation theory. Steel Compos. Struct.

2019;32(3):389-410.
Available from: https://doi.org/10.12989/scs.2019.32.3.389
10. Alibeigloo A, Alizadeh M. Static and free vibration analyses of functionally graded sandwich plates using state space differential quadrature method. Eur. J. Mech. A/Solids. 2015;54:252-66. Available from: https://doi.org/10.1016/j.euromechsol.2015.06.011
11. Natarajan S, Manickam G. Bending and vibration of functionally graded material sandwich plates using an accurate theory. Finite Elem. Anal. Des. 2012;57:32-42.
Available from: https://doi.org/10.1016/j.finel.2012.03.006
12. Li Q, Iu VP, Kou KP. Three-dimensional vibration analysis of functionally graded material sandwich plates. J. Sound Vib. 2008;311:498–515.
Available from: https://doi.org/10.1016/j.jsv.2007.09.018
13. Liu N, Jeffers AE. Isogeometric analysis of laminated composite and functionally graded sandwich plates based on a layerwise displacement theory. Compos. Struct. 2017;176(15):143-53. Available from: https://doi.org/10.1016/j.compstruct.2017.05.037
14. Neves A, Ferreira A, Carrera E, Cinefra M, Roque C, Jorge R, Soares CM. Static, free vibration and buckling analysis of isotropic and sandwich functionally graded plates using a quasi-3D higher-order shear deformation theory and a meshless technique. Compos. B: Eng. 2013;44:657-74.
Available from: https://doi.org/10.1016/j.compositesb.2012.01.089
15. Wang Y, Tham L, Cheung Y. Beams and plates on elastic foundations: a review. Prog Struct Eng Mat. 2005;7:174–82. Available from: https://doi.org/10.1002/pse.202
16. Winkler E. Die Lehre von der Elastizität und Festigkeit (The Theory of Elasticity and Stiffness), H. Dominicus, Prague, Czechoslovakia. 1867.
17. Kolahchi R, Safari M, Esmailpour M. Dynamic stability analysis of temperature-dependent functionally graded CNT-reinforced visco-plates resting on orthotropic elastomeric medium, Compos. Struct. 2016;150:255–65.
Available from: https://doi.org/10.1016/j.compstruct.2016.05.023
18. Pasternak P. On a New Method of Analysis of an Elastic Foundation by Means of Two Foundation Constants, Gosudarstvennoe Izdatelstvo Literaturi po Stroitelstvu i Arkhitekture, Moscow. 1954.
19. Kneifati MC. Analysis of plates on a Kerr foundation model. J. Eng. Mech. 1985;111:1325–42.
20. Mohamed M, Samir B, Abdelkader M, Abdelouahed T, Abdelmoumen AB, Mahmoud SR. Thermodynamic behavior of functionally graded sandwich plates resting on different elastic foundation and with various boundary conditions. J. Sandw. Struct. Mater. 2021;23(3):1028-57.
Available from: https://doi.org/10.1177/1099636219851281
21. Guerroudj HZ, Yeghnem R, Kaci A, Zaoui FZ, Benyoucef S. Eigenfrequencies of advanced composite plates using an efficient hybrid quasi-3D shear deformation theory. Smart Struct. Syst. 2018;22(1):121-32.
Available from: https://doi.org/10.12989/sss.2018.22.1.121
22. Lazreg H, Mehmet A, Nafissa Z. Natural frequency analysis of imperfect FG sandwich plates resting on Winkler-Pasternak foundation. Mater. Today: Proc. 2022;53(1):153-60.
Available from: https://doi.org/10.1016/j.matpr.2021.12.485
23. Kurpa L, Shmatko T, Linnik A. Buckling Analysis of Functionally Graded Sandwich Plates Resting on an Elastic Foundation and Subjected to a Nonuniform Loading. Mech. Compos. Mater. 2023;59:645-58. Available from: https://doi.org/10.1007/s11029-023-10122-w
24. Pham VV, Le QH. Finite element analysis of functionally graded sandwich plates with porosity via a new hyperbolic shear deformation theory. Def. Technol. 2022;18(3):490-508.
Available from: https://doi.org/10.1016/j.dt.2021.03.006
25. Dang TH, Yang DJ, Liu Y. Improvements in shear locking and spurious zero energy modes using Chebyshev finite element method. J. Comput. Inf. Sci. Eng. 2019;19:011006.
Available from: https://doi.org/10.1115/1.4041829
26. Ton-That HL, Nguyen-Van H, Chau-Dinh T. A novel quadrilateral element for analysis of functionally graded porous plates/shells reinforced by graphene platelets. Arch. Appl. Mech. 2021;91:2435-66. Available from: https://doi.org/10.1007/s00419-021-01893-6
27. Fornberg B, Zuev J. The Runge Phenomenon and Spatially Variable Shape Parameters in RBF Interpolation. Comput. Math. Appl. 2007;54(3):379–98.
Available from: https://doi.org/10.1016/j.camwa.2007.01.028
28. Lee SJ. Free Vibration Analysis of Plates by Using a Four-Node Finite Element Formulated With Assumed Natural Transverse Shear Strain. J. Sound Vib. 2004;278(3):657–84.
Available from: https://doi.org/10.1016/j.jsv.2003.10.018
29. Abassian F, Haswell DJ, Knowles NC. Free Vibration Benchmarks. National Agency for Finite Element Methods and Standards, Glasgow, UK. 1987.
30. Shahsavari D, Shahsavari M, Li L, Karami B. A novel quasi-3D hyperbolic theory for free vibration of FG plates with porosities resting on Winkler/Pasternak/Kerr foundation. Aerosp. Sci. Technol. 2018;72:134-49.
Available from: https://doi.org/10.1016/j.ast.2017.11.004
31. Baferani AH, Saidi A, Ehteshami H. Accurate solution for free vibration analysis of functionally graded thick rectangular plates resting on elastic foundation. Compos. Struct. 2011;93(7):1842-53.
Available from: https://doi.org/10.1016/j.compstruct.2011.01.020
32. Akavci S. Mechanical behaviour of functionally graded sandwich plates on elastic foundation. Compos. B: Eng. 2016;96:136-52.
Available from: https://doi.org/10.1016/j.compositesb.2016.04.035

Hoang Lan TON-THAT: https://orcid.org/0000-0002-3544-917X